JOURNAL OF SOLID STATE CHEMISTRY 120, 164–169 (1995)

Preparation and Crystal Structure Determination of $La_{20}Ti_{11}S_{44}O_6$

C. Deudon, A. Meerschaut, L. Cario, and J. Rouxel

Institut des Matériaux de Nantes, UMR-CNRS 110, Laboratoire de chimie des solides, 2, rue de la Houssinière, 44072 Nantes, Cedex 02, France

Received March 13, 1995; in revised form July 17, 1995; accepted July 20, 1995

The new quaternary oxysulfide, $La_{20}Ti_{11}S_{44}O_6$, crystallizes in the orthorhombic system, space group *Pmmn* (No. 59), $Z = 2$, $a = 22.700(5)$ Å, $b = 14.381(3)$ Å, $c = 10.454(2)$ Å. The structure was determined from a single-crystal X-ray diffraction study and led to conventional R factors, $R = 0.051$, $R_w = 0.059$ for 3264 reflections ($I > 4\ \sigma(I)$). Lanthanum atoms are engaged in mono-, bi-, or tricapped trigonal prismatic polyhedra; titanium atoms are all octahedrally coordinated. Rutile-like chains made of edge-sharing $Ti(S,O)_6$ octahedra are located in tunnels parallel to the $\vec{b}$ and $\vec{c}$ directions. © 1995 Academic Press, Inc.

INTRODUCTION

In 1975, Donohue (1) reported the existence of $LnTX_3$ compounds (with Ln = rare earth, Bi; T = Nb, Ta, Ti, V; X = S, Se). However, neither their exact chemical composition nor their structure determination were defined at that time. Recently many of these compounds have been crystallochemically characterized. Most of them belong to a wide family of misfit layer compounds with general formulation $(MX)_{1+x}(TX_2)_m$ (M = rare earth, Sn, Pb, Bi; T = Ti, V, Cr, Nb, Ta; X = S, Se; $0.08 < x < 0.3$; and m = 1, 2, 3) (see the review article (2)).

In that way, niobium (or tantalum) ternary chalcogenide compounds have been characterized and structurally determined for $M = Ln$, Sn, Pb, Bi. The chromium derivatives were only obtained when M = Bi, Ln (rare earth). In contrast, the titanium derivatives have been only studied with M = Sn, Pb, Bi, even if $LaTiS_3$ was earlier recognized (1). As examples, one can notice $[PbS]_{1+x}TiS_2$ and $[PbS]_{1+x}(TiS_2)_2$ phases ((3, 4), respectively).

Attempts to prepare the corresponding misfit phases $(LnS)_{1+x}(TiS_2)_m$ were done. In the course of these studies, we indeed identified the misfit phase $(LaS)_{1+x}TiS_2$ and, in addition, a few small crystals of a side-product structurally defined as $La_{20}Ti_{11}S_{44}O_6$. The present paper is dealing with the structure determination of this new quaternary phase.

EXPERIMENTAL

Synthesis

In order to prepare the $(LaS)_{1+x}(TiS_2)_m$ misfit compounds, the corresponding binary sulfides La_2S_3 and TiS_2 were mixed in a ratio of 1:2. The mixture was sealed in an evacuated quartz ampoule and heated at a rate of 10°C/hr to 1050°C. Besides well-crystallized black platelets corresponding to the misfit material, small crystallites with an octogonal base-shape were obtained. Semiquantitative chemical analyses on these crystallites were carried out using an electron microprobe (TRACOR dispersive energy model) mounted on a scanning electron microscope. Analyses on four crystals gave the following averaged percentages: %La = 26.86, %Ti = 14.87, %S = 58.26. By this technique, oxygen could not be "detected." Its presence was further assumed because of the too-short interatomic distances to Ti (<2.0 Å) and La (<2.6 Å) atoms. An explanation of its presence could be that the sulfidizing process of La_2O_3 was not completely achieved, which means that some traces of $La_{10}OS_{14}$ or La_2O_2S could be still present in our La_2S_3 starting material.

Symmetry and Unit Cell Parameters

Preliminary precession and Weissenberg X-ray investigations indicated that the symmetry of the structure was orthorhombic. The observed systematic conditions, $hk0$, $h + k = 2n$, $h00$, $h = 2n$, $0k0$, $k = 2n$, are compatible with the $P2_1mn$ (or $Pm2_1n$) (No. 31) and *Pmmn* (No. 59) space groups. A suitable crystal ($0.15 \times 0.07 \times 0.03$ mm^3) was mounted on an Enraf-Nonius CAD4 diffractometer for data collection using Mo$K\alpha$ radiation. Unit cell parameters were determined from 25 reflections in the range $5.4° < \theta < 22.0°$. Table I lists the cell parameters and the experimental conditions for data collection. The MOLEN program (5) was used for data reduction, absorption corrections (DIFABS program (6) in the mode that utilizes θ-dependent systematic deviations $|F_o| - |F_c|$), structure solution, and refinement.

0022-4596/95 $12.00

TABLE 1
Details of the Data Collection and Refinement Results for the Structure Determination of $La_{20}Ti_{11}S_{44}O_6$

$La_{20}Ti_{11}S_{44}O_6$; $Z = 2$	
orthorhombic symmetry, space group *Pmmn* (origin at $\bar{1}$)	
$a = 22.700(5)$ Å, $b = 14.381(3)$ Å, $c = 10.454(2)$ Å	
Temperature of measurement	293 K
Wavelength	Mo$K\alpha$, $\lambda = 0.7107$ Å
Monochromator	Graphite
ρcalc = 4.682 g cm^{-3}	
μ(cm^{-1}) = 148 cm^{-1}	
θ range	1.5°–35°
Scan ω; $\Delta\omega = 1.00 + 0.35 \tan\theta$	
Number of reflections ($I \geq 4\sigma(I)$),	$m = 3264$
Number of variables	$n = 130$
$R = 0.051$; $R_w = 0.059$	

STRUCTURE REFINEMENT

A total of 8243 unique reflections were measured within the range $0 < h < 36$, $0 < k < 23$, $0 < l < 16$, $1.5° < \theta < 35°$, of which 3809 were above the significance level of $3\sigma(I)$. Crystal stabilities were checked by monitoring intensities of three standard reflections every hour. No decay (+0.1%) was observed during the data collection period. The intensity data were corrected for Lorentz polarization effects and for absorption by an empirical method (DIFABS program (6)).

The structure was solved by Patterson and Fourier methods and refined by full-matrix least-square methods which minimized $\Sigma\, w(|F_o| - |F_c|)^2$, where $w = 4Fo^2/[\sigma(I)^2 + (0.03Fo^2)^2]$. Atomic scattering factors (neutral atoms) which included anomalous scattering contributions were from Ref. (7). The positions of La, Ti, and S atoms were first considered; then, some of the S atoms were substituted by O (oxygen) atoms in view of the too-short interatomic distances (M–S < 2 Å). Moreover, to give credit to this, these "substituted" positions showed the highest B values. Full-matrix least-squares refinement on F, anisotropic for La atoms and isotropic for the other atoms, converged to $R = 0.051$, $R_w = 0.059$ (3264 reflections $I > 4\,\sigma(I)$, 130 variables). The secondary extinction coefficient refined to $g = 1.01 \times 10^{-8}$. The final difference map showed no significant residual peak. The fractional coordinates and temperature factors (B_{eq} and B_{iso}) of all atoms with their estimated standard deviations are given in Table II. Anisotropic temperature factors of La atoms are reported in Table III.

STRUCTURE DESCRIPTION

The structure shows seven distinct La polyhedra and six Ti polyhedra. Most of the Ti polyhedra are engaged in "rutile-type chains." Indeed, the Ti(1), Ti(2), and Ti(3) edge-shared octahedra form a first chain along the $\vec{c}$ direction, Ti(4) and Ti(5) edge-shared octahedra forming the second one along the $\vec{b}$ direction (see Fig. 1). The remaining Ti(6) atoms are engaged in an isolated double octahedra (O(3) corner-sharing) which bridge two La(7) atoms.

The La(1) and La(3) atoms are coordinated by the seven nearest sulfurs located at the corners of a monocapped triangular prism. La–S distances within both polyhedra are

TABLE 2
Positions and Thermal Parameters

Atom	Site	x	y	z	$B_{eq,iso}$* (Å^2)
La1	4(*f*)	0.66046(7)	1/4	0.6355(1)	0.91(2)
La2	8(*g*)	0.16410(4)	0.03749(6)	0.36391(8)	0.44(1)
La3	4(*f*)	0.65900(6)	1/4	0.0475(1)	0.44(2)
La4	8(*g*)	0.16058(4)	0.04074(6)	0.95069(8)	0.39(1)
La5	4(*f*)	0.03423(8)	1/4	0.6125(1)	0.91(2)
La6	8(*g*)	0.03092(4)	0.55490(6)	0.66645(9)	0.58(1)
La7	4(*f*)	0.03321(7)	1/4	0.0737(1)	0.72(2)
Ti1	2(*a*)	1/4	1/4	0.8588(6)	0.44(8)*
Ti2	2(*a*)	1/4	1/4	0.1583(7)	0.38(7)*
Ti3	2(*a*)	1/4	1/4	0.4569(6)	0.32(8)*
Ti4	4(*e*)	1/4	0.8674(3)	0.6641(5)	0.64(6)*
Ti5	4(*e*)	1/4	0.0983(3)	0.6612(4)	0.38(5)*
Ti6	8(*g*)	0.0624(1)	0.8816(2)	0.1560(3)	0.52(4)*
S1	8(*g*)	0.0747(2)	0.0599(3)	0.1611(4)	0.45(5)*
S2	4(*f*)	0.1684(3)	1/4	0.3200(5)	0.48(8)*
S3	4(*f*)	0.1732(3)	3/4	0.6613(7)	0.71(8)*
S4	4(*e*)	1/4	0.8853(4)	0.4322(5)	0.40(8)*
S5	4(*f*)	0.1658(3)	1/4	0.0017(5)	0.36(7)*
S6	8(*g*)	0.1700(2)	0.8836(3)	0.1581(4)	0.54(5)*
S7	4(*f*)	0.1816(2)	1/4	0.6613(6)	0.37(7)*
S8	8(*g*)	0.0687(2)	0.8802(3)	0.3885(4)	0.57(6)*
S9	8(*g*)	0.0700(2)	0.8871(3)	0.9222(4)	0.51(6)*
S10	4(*f*)	0.9882(3)	1/4	0.3299(6)	0.64(8)*
S11	8(*g*)	0.0435(2)	0.1195(3)	0.8395(4)	0.45(5)*
S12	8(*g*)	0.0661(2)	0.0885(3)	0.4986(5)	0.73(6)*
S13	8(*g*)	0.1706(2)	0.9917(3)	0.6658(4)	0.50(5)*
S14	4(*e*)	1/4	0.8866(4)	0.8943(6)	0.49(8)*
S15	4(*e*)	1/4	0.0807(4)	0.1537(6)	0.43(7)*
O1	4(*e*)	1/4	0.113(1)	0.475(1)	0.4(2)*
O2	4(*e*)	1/4	0.114(1)	0.847(2)	0.3(2)*
O3	4(*f*)	0.0641(8)	3/4	0.143(2)	1.0(3)*

Note. Standard deviations are given in parentheses.

TABLE 3
Anisotropic Temperature Factors of La Atoms

	$U(1,1)$	$U(2,2)$	$U(3,3)$	$U(1,2)$	$U(1,3)$	$U(2,3)$
La1	0.0152(6)	0.0046(5)	0.0149(7)	0	0.0016(6)	0
La2	0.0069(3)	0.0043(3)	0.0056(4)	−0.0007(3)	−0.0014(3)	0.0003(3)
La3	0.0074(5)	0.0038(5)	0.0057(5)	0	−0.0020(5)	0
La4	0.0076(3)	0.0038(3)	0.0033(3)	−0.0002(4)	0.0002(3)	−0.0006(3)
La5	0.0183(7)	0.0063(5)	0.0100(6)	0	−0.0033(6)	0
La6	0.0125(3)	0.0069(3)	0.0028(3)	0.0024(3)	−0.0011(4)	−0.0006(4)
La7	0.0123(6)	0.0038(5)	0.0111(6)	0	0.0053(6)	0

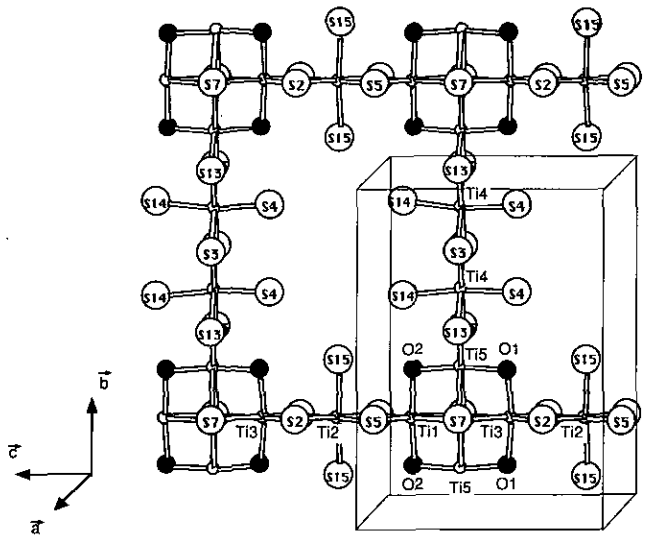

FIG. 1. Edge-shared Ti octahedra developing into rutile chains parallel to the $\vec{b}$ and $\vec{c}$ directions (all at $x = 1/4$).

quite comparable (average distances, La(1)–S = 2.932 Å and La(3)–S = 2.940 Å; the longest La–S distance in each polyhedron corresponds to the monocapped S atom). One can notice that an oxygen atom, O(3), is in the close surroundings of La(1) and La(3) atoms, 3.188 and 2.929 Å, respectively. These polyhedra develop into a double chain, running in the $\vec{c}$ direction, by sharing, alternately, corners (S(3)) and edges (S(6)–S(6)) (see Fig. 2). Such an entity leaves 1D channels (parallel to the $\vec{b}$ direction) in which the rutile chain, constituted by the infinite Ti(4)–Ti(4)–Ti(5) sequence, is located.

La(2) and La(4) polyhedra are bicapped and tricapped

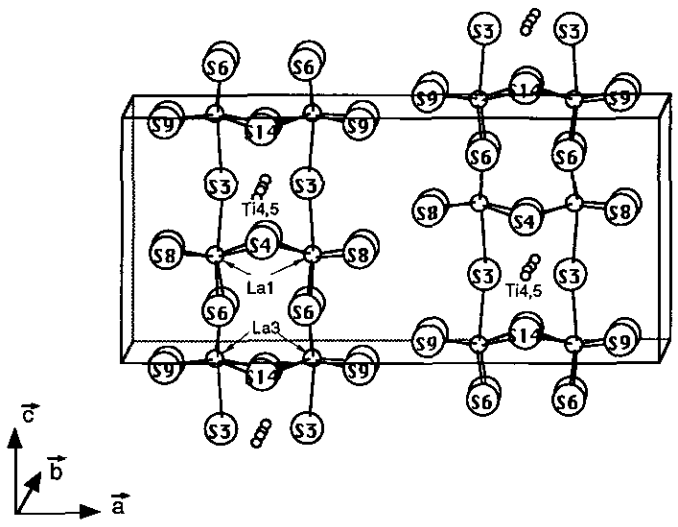

FIG. 2. Edge- and corner-shared La(1)–La(3) polyhedra; Ti atoms engaged in the rutile chain ∥ to $\vec{b}$ are indicated by open circles.

trigonal prisms, respectively. There is one oxygen atom among the nearest neighboring atoms of these two La atoms. Four La(2) and four La(4) polyhedra are linked together to build a new structural unit in which a tunnel is developed in the $\vec{c}$ direction. This entity consists of a planar association (parallel to the (*a*, *b*) plane) of 4 La(2) polyhedra separated by 4 La(4) polyhedra; La(2) polyhedra are linked together by sharing either a triangular face (S(4), S(15), O(1)) or a common corner S(2) (see Fig. 3a); a similar situation occurs in the plane of the 4 La(4) polyhedra, i.e., La(4) polyhedra are associated by sharing either a triangular face ((S(14), S(15), O(2)) or a corner (S(5)) (see Fig. 3b). The connection between planes of La(2) and La(4) polyhedra is made through a triangular face (S(15), S(6), S(1)). In this "hollowed" entity, the second rutile chain made of Ti(1)–Ti(2)–Ti(3) edge-shared polyhedra is taking place.

The three last polyhedra (around La(5), La(6), La(7)) are closely packed to form layers parallel to the (*b*, *c*) plane (see Fig. 4). The number of close neighbor atoms coordinated to La atoms in these polyhedra ranges from 7 for La(5) to 8 for La(7).

As mentioned above, rutile chains are running along either $\vec{b}$ (Ti(4), Ti(5)) or $\vec{c}$ (Ti(1), Ti(2), Ti(3)) directions. Rather short Ti–Ti distances are observed within these chains. Thus, in the rutile chain parallel to the $\vec{c}$ direction, two distances of 3.13 Å (Ti(1)–Ti(2)) and 3.12 Å (Ti(2)–Ti(3)) are separated by a longer one (Ti(3)–Ti(1) = 4.20 Å). Similarly, two short Ti–Ti distances separated by a longer one are also encountered within the rutile chain developing parallel to the $\vec{b}$ direction, viz. Ti(4)–Ti(4) = 3.38 Å, Ti(4)–Ti(5) = 3.32 Å and Ti(5)–Ti(5) = 4.36 Å.

The longest Ti–Ti distances, along both rutile chains, occur between Ti atoms engaged in a squared cluster (Ti(1), Ti(3), 2 Ti(5)), at the cross-over of the rutile chains (see Fig. 1). However, in this cluster, one notices rather short Ti–Ti distances between atoms of separate rutile chains (i.e., Ti(1)–Ti(5) = 3.004 Å and Ti(3)–Ti(3) = 3.053 Å). S(7) atoms are shared by the four Ti atoms of the cluster, thus leading to Ti–S(7) distances longer than other Ti–S ones. The cross-over between Ti polyhedra is established around Ti(1)–Ti(3) ($\vec{c}$ chain direction) and Ti(5)–Ti(5) ($\vec{b}$ chain direction). Triangular face-sharing (S(7)–S(7)–O(2)) between Ti(1) and Ti(5) octahedra, and (S(7)–S(7)–O(1)) between Ti(3) and Ti(5) polyhedra are taking place. Finally, the last metal atom, Ti(6), which is engaged in a double octahedra connected via the O(3) atom, does not belong to any rutile chain. These double octahedra connect adjacent La(5)–La(6)–La(7) planes (see Fig. 4).

Table IV summarizes the main interatomic distances within the various La and Ti polyhedra. It can be noticed that rather short La–S(12) distances are found (La(2)–S(12) = 2.732 Å, La(5)–2S(12) = 2.709 Å and La(6)–

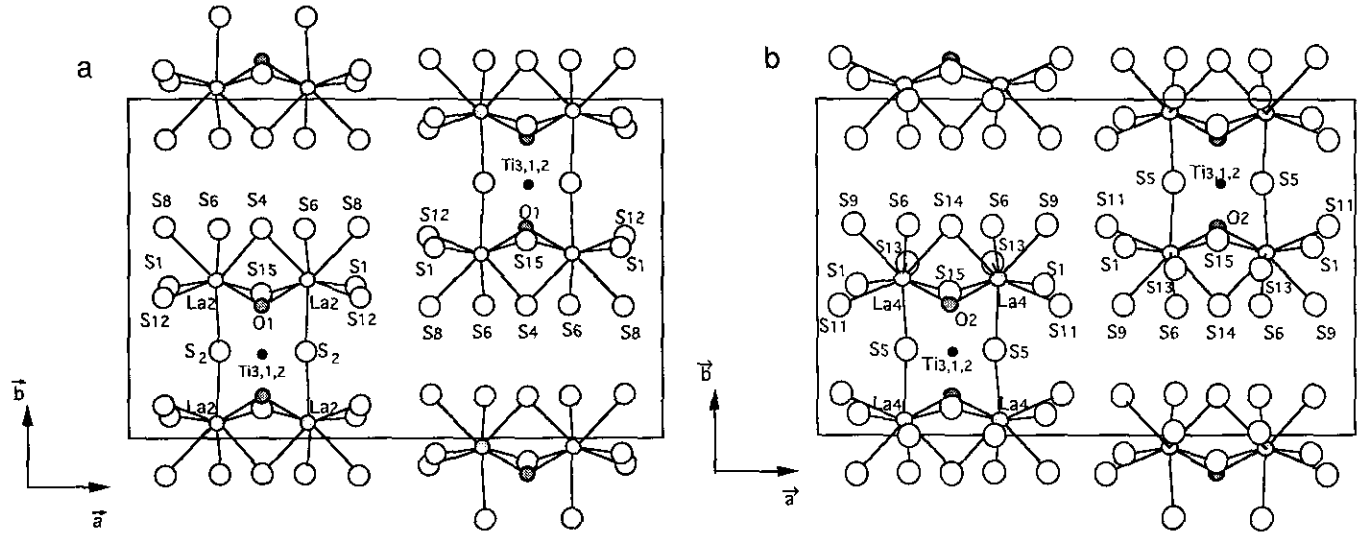

FIG. 3. (a) Detailed environment around La(2), $z = 0.36$. (b) Detailed environment around La(4), $z = 0.95$.

S(12) = 2.840 Å). A partial sulfur oxygen substitution was tested upon refinement with constrained positional parameters and a multiplicity factor on both atoms. No improvement was observed, the refined multiplicity converging to 0.93(2) for S and then to 0.07 for O.

DISCUSSION AND CONCLUDING REMARKS

The presence of oxygen in this compound was assumed in the last stage of the refinement in the light of the too-short La–S (<2.6 Å) or Ti–S (<2.0 Å) distances. This led to the substitution of three atomic positions initially occupied by S atoms by three oxygen atoms (O(1), O(2), O(3)) (see Table IV). All the other M–S distances are compatible with La–S or Ti–S distances reported in the literature. Ti octahedra are slightly distorted, those belonging to the rutile chain parallel to $\vec{c}$ (Ti(1), Ti(2), Ti(3)) being more distorted than those of the rutile chain parallel to $\vec{b}$ (Ti(4), Ti(5)). For example, the S–Ti(2)–S angles range between 83° and 98° for the Ti(1) octahedron while the range angle is 85–95° for the Ti(4) octahedron (see Table V). Such a distortion could be expected if a Jahn–Teller effect, intrinsic to the Ti^{3+} cation, was occurring. In such a case, the Jahn–Teller effect should be mainly observed in the Ti–(S, O) bond length variation; from the list of Ti–(S, O) distances (Table IVb), no significant evidence of this effect is noticed.

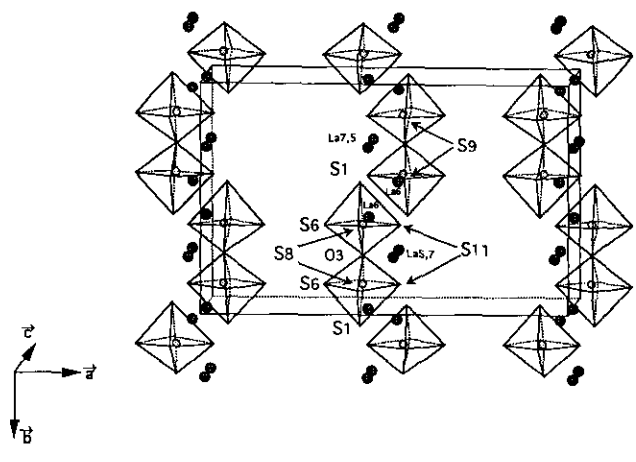

FIG. 4. Isolated corner-shared Ti(6) octahedra developing in layers parallel to the (b, c) plane; La(5), La(6), and La(7) atoms are pointed out.

From a charge equilibrium point of view, considering the chemical composition as deduced from this crystal structure study, $La_{20}Ti_{11}S_{44}O_6$, 100 negative charges have to be balanced by as many positive ones. Sixty positive charges are coming from La (assuming La^{3+}) and 40 positive ones should come from 11 Ti, which can be at the +3 or +4 oxidation states. Thus, the question arises about the location of Ti^{3+} and Ti^{4+} in the structure. Clearly Ti^{3+} could be represented by Ti(4) and Ti(2), which are surrounded only by sulfur, the less electronegative anionic species. As there are 2 Ti(4) and one Ti(2) this brings 9 positive charges. Other titanium (1 Ti(1), 1 Ti(3), 2 Ti(5), and 4 Ti(6)) would bring 32 charges. A total of 41 positive charges would result. Now, another possibility refers to what has been found in the so-called Magneli phases Ti_nO_{2n-1}, where Ti^{3+} is located in shear planes involving octahedra sharing faces between rutile blocks. Here, rutile chains are connected by octahedra sharing faces involving a group of four titanium atoms, (Ti(1), Ti(3), and 2 Ti(5)), constituting what could be called a shear knot.

Assuming these titanium to be Ti^{3+}, it gives 12 positive charges. The remaining titanium (1Ti(2), 2 Ti(4), and 4

TABLE 4
Interatomic Distances (Å)

		a	
La–S3	3.117(8)	La3–S3	3.061(8)
La1–2S4	2.902(5)	La3–2S6	2.894(4)
La1–2S6	2.897(4)	La3–2S9	2.840(5)
La1–2S8	2.811(5)	La3–2S14	2.915(5)
[La1–O3	3.188(2)]	[La3–O3	2.930(19)]
(La1–S)average	2.932	(La3–S)average	2.940
La2–S1	2.953(4)	La4–S1	2.952(4)
La2–S2	3.092(1)	La4–S5	3.059(1)
La2–S4	3.017(5)	La4–S6	3.139(4)
La2–S6	3.089(4)	La4–S9	3.032(5)
La2–S8	3.142(5)	La4–S11	3.114(4)
La2–S12	2.732(5)	La4–S13	3.069(5)
La2–S15	3.003(5)	La4–S14	3.063(5)
La2-O1	2.518(11)	La4–S15	2.993(5)
[La2–S13	3.227(5)]	La4–O2	2.532(10)
(La2/S)average	3.147	(La4–S)average	3.053
La5–2S8	2.994(5)	La6–S1	3.001(4)
La5–S10	3.134(7)	La6–S8	3.170(5)
La5–2S11	3.033(4)	La6–S9	2.938(5)
La5–2S12	2.709(4)	La6–S10	2.839(1)
(La5–S)average	2.968	La6–S11	3.106(4)
		La6–S12	2.840(5)
La7–2S1	3.032(4)	La6–S12	2.823(5)
La7–S5	3.102(7)	La6–S13	3.240(4)
La7–2S9	3.063(5)	(La6–S)average	3.019
La7–S10	2.866(7)		
La7–2S11	3.094(4)		
(La7–S)average	3.031		
		b	
Ti1–2O2	1.954(15)	Ti2–2S2	2.507(8)
Ti1–2S5	2.426(7)	Ti2–2S5	2.517(8)
Ti1–2S7	2.584(8)	Ti2–2S15	2.434(5)
(Ti1–S)average	2.505	(Ti2–S)average	2.486
Ti3–2O1	1.972(17)	Ti4–2S3	2.428(5)
Ti3–2S2	2.341(7)	Ti4–S4	2.437(8)
Ti3–2S7	2.641(8)	Ti4–2S13	2.539(5)
(Ti3–S)average	2.491	Ti4–S14	2.422(8)
		(Ti4–S)average	2.466
Ti5–O1	1.961(18)	Ti6–O3	1.898(3)
Ti5–O2	1.959(19)	Ti6–S1	2.580(5)
Ti5–2S7	2.678(4)	Ti6–S6	2.444(4)
Ti5–2S13	2.366(4)	Ti6–S8	2.435(6)
(Ti5–S)average	2.522	Ti6–S9	2.451(6)
(Ti5–O)average	1.96	Ti6–S11	2.405(5)
		(Ti6–S)average	2.463

Note. Standard deviations are given in parentheses.

TABLE 5
Interatomic Ti–Ti Distances (Å) and S–Ti–S Angles (°)

Ti(1)–Ti(2)	3.131(10)	Ti(4)–Ti(4)	3.377(8)
Ti(2)–Ti(3)	3.121(10)	Ti(4)–Ti(5)	3.320(6)
Ti(3)–Ti(1)	4.201(8)	Ti(5)–Ti(5)	4.364(8)
	Ti(1)–Ti(5)	3.004(6)	
	Ti(3)–Ti(5)	3.053(6)	
S(2)–Ti(2)–S(2)	95.24(37)	S(3)–Ti(4)–S(3)	91.85(24)
S(2)–Ti(2)–S(5)	82.96(17)	S(3)–Ti(4)–S(13)	88.83(12)
S(5)–Ti(2)–S(5)	98.84(37)	S(13)–Ti(4)–S(13)	90.48(22)
S(2)–Ti(2)–S(15)	90.77(16)	S(3)–Ti(4)–S(4)	93.54(26)
S(5)–Ti(2)–S(15)	89.26(16)	S(13)–Ti(4)–S(4)	86.14(20)
		S(3)–Ti(4)–S(14)	95.23(26)
		S(13)–Ti(4)–S(14)	84.99(20)

Ti(6)) would bring 28 charges. The total reaches the expected value of 40. The latter hypothesis is also supported by the fact that the titanium at the knots see each other through the common face of their coordination polyhedra. All other titanium atoms share edges or corners. The bond valence method (8) did not show any significant distinction (see Table VI). One can add that the bond valence calculations show that oxygen atoms are closer to 2^- if Ti(1), Ti(3), and Ti(5) are taken at the 3^+ oxidation state rather than 4^+. It does not seem possible to proceed further in that discussion at present. In addition only a few very small crystals were obtained, which does not allow physical measurements to be performed.

This oxysulfide quaternary compound is by no means an intermediate phase between La_2TiO_5 and La_2TiS_5. Although the ternary oxide compound is well known (9), the corresponding sulfide derivative is, up to now, unknown. The structure arrangement is very unique, with rutile chains that run perpendicular to each other and are connected through a very particular condensation of Ti(O, $S)_6$ octahedra.

Very recently refinements of two other lanthanum titanium oxisulfides (10) have been published. These phases, with composition $La_6Ti_2S_8O_5$ and $La_4Ti_3S_4O_8$, show totally different structural arrangements.

TABLE 6
Bond Valence (γ_{ij}) Distribution of Ti Atoms

Atom	Ti(1)	Ti(2)	Ti(3)	Ti(4)	Ti(5)	Ti(6)
Ti^{3+}	3.33		3.42		3.30	3.52
		3.10		3.29		
Ti^{4+}	3.37		3.51		3.39	3.57

Note. The bond valences (γ_{ij}) were calculated from the expression $\gamma_{ij} = \exp[(r_0 - d_{ij})/b]$, where $b = 0.37$ and $r_0(Ti^{3+} - O) = 1.791$, $r_0(Ti^{4+} - O) = 1.815$, $r_0(Ti-S) = 2.24$, and d_{ij} are the interatomic distances (Table IVb).

REFERENCES

1. P. C. Donohue, *J. Solid State Chem.* **12,** 80–83 (1975).
2. G. A. Wiegers and A. Meerschaut, *in* "Incommensurate Sandwiched Layered Compounds" (A. Meerschaut, Ed.), pp. 101–172. Trans Tech Pub. (1992).
3. S. van Smaalen, A. Meetsma, G. A. Wiegers, and J. L. de Boer, *Acta Crystallogr. B* **47**(3), 314–330 (1991); S. van Smaalen and J. L. de Boer, *Phys. Rev. B* **46**(5), 2750–2757 (1992).
4. A. Meerschaut, C. Auriel, and J. Rouxel, *J. Alloys Comp.* **183,** 129–137 (1992).
5. C. Kay Fair, "MOLEN Structure Determination Package," Enraf-Nonius, Delft, The Netherlands, 1990.
6. N. Walker and D. Stuart, *Acta Crystallogr A* **39,** 158–166 (1983).
7. "International Tables for X-Ray Crystallography" Vol. IV. Kynoch Press, Birmingham, England, 1974.
8. N. E. Brese and M. O'Keeffe, *Acta Crystallogr. B* **47,** 192–197 (1991).
9. M. Guillen and E. F. Bertaut, *Bull. Soc. Fr. Ceram.,* 7257 (1966).
10. J. A. Cody and J. A. Ibers, *J. Solid State Chem.* **114,** 406–412 (1995).